Various high-order modes in vertical-cavity surface-emitting lasers with equilateral triangular lateral confinement

C. C. Chen, K. W. Su, Y. F. Chen,* and K. F. Huang

Department of Electrophysics, National Chiao Tung University, Hsinchu, Taiwan
**Corresponding author: yfchen@cc.nctu.edu.tw*

Received December 6, 2007; accepted January 18, 2008;
posted January 30, 2008 (Doc. ID 90598); published February 28, 2008

Large-aperture vertical-cavity surface-emitting lasers with an equilateral triangular lateral confinement are fabricated to investigate the formation of high-order resonant modes. The experimental lasing patterns are composed of the superscar mode, honeycomb eigenstate, and chaotic mode. Experimental results confirm the theoretical predictions that tiny symmetry breaking can cause the high-order modes to reveal miscellaneous states of integrable and chaotic systems. © 2008 Optical Society of America

OCIS codes: 140.3410, 140.5960, 300.6260.

Microdisk lasers with chaotic shapes permit high-power directional emission and have potential applications in optical computations and communications [1–3]. The lasing mechanism of directional emission in chaotic microdisk lasers has been analogously interpreted with the scar effect in chaotic billiards [4]. Specifically, scar modes have the wave patterns to be localized on the isolated and unstable periodic orbits (POs) in the chaotic quantum billiards [4]. In addition to scar modes, the other significant high-order states are the so-called superscar modes [5] that are localized on stable and nonisolated POs. Superscar modes have been theoretically studied in square [6], equilateral-triangular [7], and circular quantum billiards [8]. Recently, two-dimensional (2D) microdisk lasers have been experimentally employed to explore the characteristics of resonant modes in square [9] and equilateral-triangular [10,11] cavities. The lateral radiation patterns of 2D microdisk lasers have been found to be intimately related to the superscar modes. Nevertheless, the whole morphology of superscar modes cannot be straightforwardly observed from the lateral radiation of 2D microdisk lasers.

More recently, it has been shown that the transverse modes of the oxide confined vertical-cavity surface-emitting lasers (VCSELs) are equivalent to the wave functions in the 2D quantum billiards with the shapes the same as the lateral confinements [12–14]. The superiority of oxide-confined VCSELs consists in their longitudinal wave vector k_z, which can bring out the near-field patterns to be directly reimaged with simple optics. Although square-shaped VCSELs have been manufactured to confirm the superscar modes [13], equilateral-triangular-shaped VCSELs have not been implemented as yet. Since the equilateral-triangular billiard is a classically nonseparable but integrable system, experimental realization of the resonance modes in equilateral-triangular VCSELs can provide important insight into laser physics [15] as well as electron transport phenomena in quantum dots [16].

In this work, we fabricate large-aperture equilateral-triangular VCSELs to explore the near-field transverse patterns of the VCSELs at lasing threshold. Various high-order coherent stationary modes, including superscar modes, high-order eigenstates, and chaotic modes are experimentally observed via precise temperature control to detune the transverse order. Experimental results revealed that spontaneous imperfections cause the lasing modes of large-aperture equilateral-triangular VCSELs to exhibit miscellaneous states of integrable and chaotic systems. The fundamental operation of the large-aperture VCSELs is discussed in [13].

The device structure of the present oxide-confined VCSELs and the methods used to measure the far- and near-field patterns are similar to those described by [12], except that the lateral confinement is equilateral triangular. Figure 1 shows the optical microscope image of the device operated with an electric current under threshold current at room temperature. The bright region indicates the equilateral-triangular pattern of spontaneous emission. The edge length of the oxide aperture was measured to be approximately 66.8 μm. The VCSEL device was placed in a cryogenic system with a temperature stability of

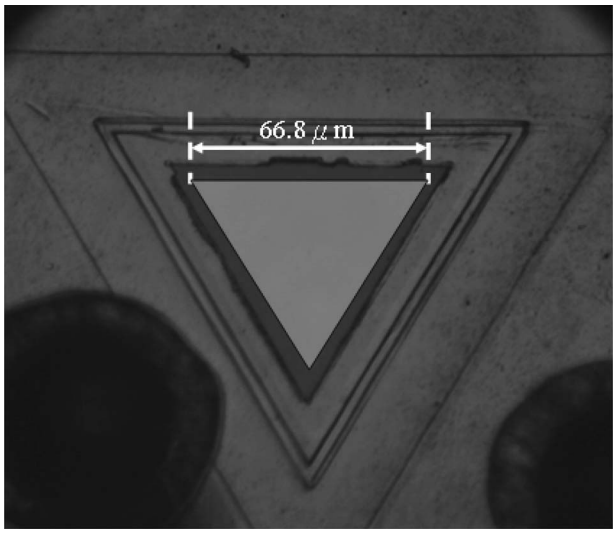

Fig. 1. Optical microscope image of the device with pattern of spontaneous emission to display the equilateral-triangular aperture.

0146-9592/08/050509-3/$15.00

0.01 K in the range of 80–300 K. A current source with a precision of 0.01 mA was utilized to drive the VCSEL device. The near-field patterns were reimaged into a CCD camera (Coherent, Beam-Code) with an objective lens (Mitsutoyo, numerical aperture 0.9). The spectral information in the laser output was measured by a Fourier optical spectrum analyzer (Advantest Q8347) with a Michelson interferometer.

Figures 2(a)–2(f) depict the experimental near-field patterns that are characteristically observed at different device temperatures. It is found that the lasing patterns are generally robust and reproducibly observed under the same experimental circumstances. The lasing pattern shown in Fig. 2(a) is obtained at the operating temperature of 295 K, and the optical spectrum indicates it to be a multimode emission. The lasing state at the operating temperature of 275 K is found to dramatically change to a superscar mode that is similar to Fabry–Pérot modes impinging on lateral sides vertically [17], as seen in Fig. 2(b). When the operating temperature decreases to 195 K, the lasing pattern shown in Fig. 2(c) exhibits a honeycomb structure. As discussed later, the honeycomb morphology corresponds to the pattern of a kind of eigenstate. When the operating temperature further decreases to 175 K, the near-field pattern shown in Fig. 2(d) behaves like a chaotic wave state that can be described as a random superposition of plane waves [18]. For the operating temperature below 135 K, the experimental pattern shown in Fig. 2(f) corresponds to another superscar mode that is related to a geometrical PO [10]. This superscar mode is found to be unchanged when the temperature decreases from 135 to 80 K. Intriguingly, the lasing pattern displays the transition and coexistence of the chaotic and superscar modes for the operating temperature within the range of 135–155 K, as seen in Fig. 2(e).

The analogy between the electromagnetic wave equation in paraxial approximation and the Schrödinger equation enables us to make a detailed connection between the quantum wave functions and the experimental patterns. Setting the three vertices to be at (0,0), $(a/2, \sqrt{3}a/2)$, and $(-a/2, \sqrt{3}a/2)$, where a is the side length, the quantum eigenstates of the equilateral-triangular billiard are given by [7]

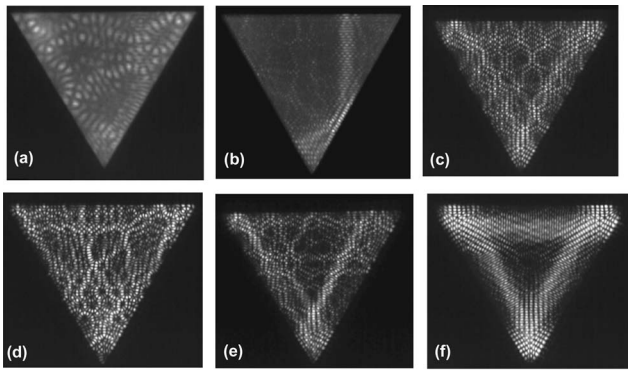

Fig. 2. Intensity patterns of transerse near-field patterns at temperatures of (a) 295 (room temperature), (b) 275, (c) 195, (d) 175, (e) 155, and (f) 125 K.

$$\Phi^{\pm}_{m,n}(x,y) = \sqrt{\frac{16}{a^2 3\sqrt{3}}}\Bigg\{ e^{\pm i(m+n)(2\pi/3a)x} \times \sin\left[(m-n)\frac{2\pi}{\sqrt{3}a}y\right] + e^{\mp i(2m-n)(2\pi/3a)x}\sin\left[n\frac{2\pi}{\sqrt{3}a}y\right] - e^{\mp i(2n-m)(2\pi/3a)x}\sin\left[m\frac{2\pi}{\sqrt{3}a}y\right]\Bigg\}, \quad (1)$$

with $2n \geq m$. The eigenstates $\Phi^{\pm}_{m,n}(x,y)$ are the representation of traveling waves. The wave functions for standing waves can be expressed as $S^{\pm}_{m,n}(x,y) = \Phi^{+}_{m,n}(x,y) \pm \Phi^{-}_{m,n}(x,y)$. The experimental honeycomb pattern shown in Fig. 2(c) can be numerically confirmed to correspond to the wave intensity of $|S^{-}_{5,58}(x,y)|^2$, as depicted in Fig. 3(a).

Superscar modes that are associated with classical POs can be analytically expressed with the representation of quantum coherent states. The formation of classical POs in the equilateral-triangular billiard can be denoted by three parameters (p,q,ϕ), where the parameters p and q are nonnegative integers with the restriction that $p \geq q$; the parameter ϕ is in the range of $-\pi$ to π [7]. With the representation of quantum coherent states, the wave functions related to the classical POs with parameters (p,q,ϕ) can be given by [7]

$$\Psi^{\pm}_{N,M}(x,y;p,q,\phi) = \frac{1}{\sqrt{M}}\sum_{K=0}^{M-1} e^{\pm iK\phi}\Phi^{\pm}_{m_o+pK,n_o+q(M-1-K)}(x,y), \quad (2)$$

with $m_o = (p+2q)N$ and $n_o = (2p+q)N$, where m_o and n_o indicate the order of the coherent state and M stands for the number of eigenstates that are involved in the superposition. The relative phase factor ϕ between various parts of the coherent state has a causal relationship with the localization on geometrical trajectories [6,7]. Similarly, $\Psi^{\pm}_{N,M}(x,y;p,q,\phi)$ represents the traveling wave, and the expression for the standing wave can be given by $C^{\pm}_{N,M}(x,y,p,q,\phi) = \Psi^{+}_{N,M}(x,y,p,q,\phi) \pm \Psi^{-}_{N,M}(x,y,p,q,\phi)$. Based on thorough numerical analysis, the experimental superscar modes can be found to be well reconstructed with the coherent states of $C^{+}_{36,9}(x,y;1,01,0.23\pi)$ and $C^{+}_{22,6}(x,y;1,1,0.35\pi)$. Figures 3(b) and 3(c) depict the numerical wave patterns of $|C^{+}_{36,9}(x,y;1,0,0.23\pi)|^2$ and $|C^{+}_{22,6}(x,y;1,1,0.35\pi)|^2$ corresponding to the experimental patterns shown in Figs. 2(b) and 2(f). The excellent agreement between the experimental and numerical patterns confirms that the quantum formulism is of great importance in describing distinct branches of physics because of the underlying structural similarity. Conversely, the present analysis also provides a further indication that laser resonators can be designed to demonstrate the quantum phenomenon in mesoscopic physics.

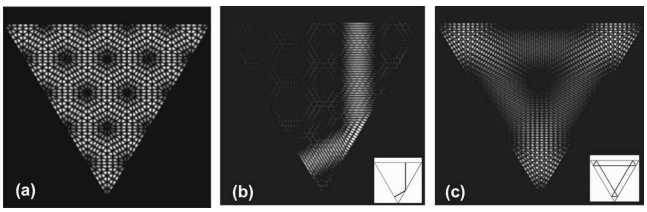

Fig. 3. (a) Numerical wave pattern $|S^{-}_{5,58}(x,y)|^2$ corresponding to the experimental honeycomb pattern shown in Fig. 2(c). (b), (c) Numerical wave patterns of $|C^{+}_{36,9}(x,y;1,0,0.23\pi)|^2$ and $|C^{+}_{22,6}(x,y;1,1,0.35\pi)|^2$ corresponding to the experimental patterns shown in Figs. 2(b) and 2(f), respectively. The geometrical POs are shown in the insets.

Although an ideal equilateral-triangular billiard is integrable, some experimental patterns reveal the property of quantum chaotic modes, as seen in Fig. 2(d). It is well known that the intensity statistics of chaotic wave functions obey the Porter–Thomas distribution $P(I)=(1/\sqrt{2\pi I})e^{-I/2}$ [19]. The intensity statistics for Fig. 2(d) can be derived by digitizing the image file with the background removal of spontaneous emission. We evaluate the intensity statistics for the experimental pattern to make a comparison with the Porter–Thomas distribution, as shown in Fig. 4. The good agreement validates that the wave pattern corresponds to a chaotic wave function. The origin of stationary chaotic modes is expected to arise from spontaneous imperfections, such as boundary roughness or inequality of the three internal angles. In other words, spontaneous symmetry breaking may cause the real devices with idealized integrable confinements to exhibit the characteristics of nonintegrable systems. As discussed in [20], although a triangular billiard with internal angles slightly different from $\pi/3$ is intrinsically chaotic, the wave functions can still be scarred by families of POs. Briefly, tiny symmetry breaking can lead to the emergence of superscar as well as chaotic modes in the almost integrable systems. Our experimental results are consistent with the theoretical findings.

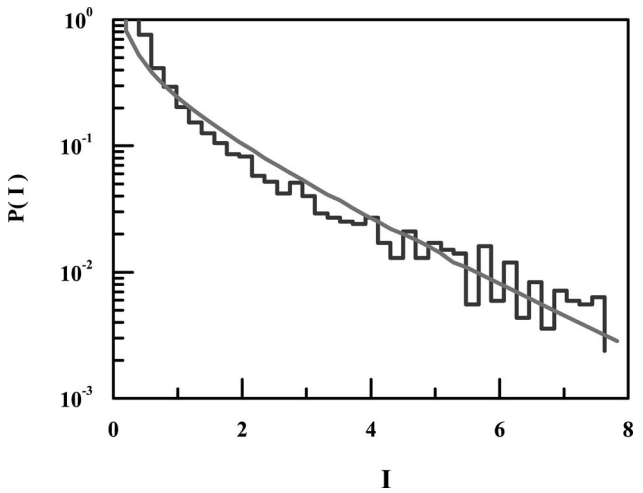

Fig. 4. Histogram: intensity statistics of the experimental pattern shown in Fig. 2(d); straight curve, Porter–Thomas distribution.

In conclusion, we have manufactured large-aperture VCSEL devices with an equilateral-triangular lateral confinement to explore the characteristics of mesoscopic resonant modes via precise temperature control. Experimental results generally confirm the theoretical predictions that spontaneous symmetry breaking can induce the appearance of superscar modes and chaotic waves. We also observed the honeycomb pattern that corresponds to the structure of a high-order eigenstate. More importantly, the experimental lasing mode within a rather wide temperature range is found to be the coexistence of superscar and chaotic states. The present result can provide useful insight into laser physics and wave chaos.

References

1. C. Gmachl, F. Capasso, E. E. Narimanov, J. U. Nöckel, A. D. Stone, J. Faist, D. L. Sivco, and A. Y. Cho, Science **280**, 1556 (1998).
2. N. B. Rex, H. E. Tureci, H. G. L. Schwefel, R. K. Chang, and A. D. Stone, Phys. Rev. Lett. **88**, 094102 (2002).
3. M. Lebental, J. S. Lauret, J. Zyss, C. Schmit, and E. Bogomolny, Phys. Rev. A **75**, 033806 (2007).
4. E. J. Heller, Phys. Rev. Lett. **53**, 1515 (1984).
5. E. Bogomolny, B. Dietz, T. Friedrich, M. Miski-Oglu, A. Richter, F. Schäfer, and C. Schmit, Phys. Rev. Lett. **97**, 254102 (2006).
6. Y. F. Chen, K. F. Huang, and Y. P. Lan, Phys. Rev. E **66**, 066210 (2002).
7. Y. F. Chen and K. F. Huang, Phys. Rev. E **68**, 066207 (2003).
8. C. C. Liu, T. H. Lu, Y. F. Chen, and K. F. Huang, Phys. Rev. E **74**, 046214 (2006).
9. A. W. Poon, F. Courvoisier, and R. K. Chang, Opt. Lett. **26**, 632 (2001).
10. H. C. Chang, G. Kioseoglou, E. H. Lee, J. Haetty, M. H. Na, Y. Xuan, H. Luo, and A. Petrou, Phys. Rev. A **62**, 013816 (2000).
11. J. Yoon, S.-J. An, K. Kim, J. K. Ku, and O. Kwon, Appl. Opt. **46**, 2969 (2007).
12. S. P. Hegarty, G. Huyet, J. G. McInerney, and K. D. Choquette, Phys. Rev. Lett. **82**, 1434 (1999).
13. K. F. Huang, Y. F. Chen, H. C. Lai, and Y. P. Lan, Phys. Rev. Lett. **89**, 224102 (2002).
14. T. Gensty, K. Becker, I. Fischer, W. Elsäßer, C. Degen, P. Debernardi, and G. P. Bava, Phys. Rev. Lett. **94**, 233901 (2005).
15. Y. Z. Huang, Y. H. Hu, Q. Chen, S. J. Wang, Y. Du, and Z. C. Fan, IEEE Photon. Technol. Lett. **19**, 963 (2007).
16. L. Christensson, H. Linke, P. Omling, P. E. Lindelof, I. V. Zozoulenko, and K. F. Berggren, Phys. Rev. B **57**, 12306 (1997).
17. J. C. Marinace, A. E. Michel, and M. I. Nathan, Proc. IEEE **52**, 722 (1964)
18. P. O'Connor, J. Gehlen, and E. J. Heller, Phys. Rev. Lett. **58**, 1296 (1987).
19. H. J. Stöckmann, *Quantum Chaos: an Introduction* (Cambridge U. Press, 1999), and references cited therein.
20. P. Bellomo and T. Uzer, Phys. Rev. E **50**, 1886 (1994).